HHS Public Access

Author manuscript

Burns. Author manuscript; available in PMC 2017 February 01.

Published in final edited form as:

Burns. 2016 February ; 42(1): 112–122. doi:10.1016/j.burns.2015.10.026.

Differential acute and chronic effects of burn trauma on murine skeletal muscle bioenergetics

Craig Porter[1,2], **David N. Herndon**[1,2], **Nisha Bhattarai**[1,2], **John O. Ogunbileje**[1,2], **Bartosz Szczesny**[3], **Csaba Szabo**[3], **Tracy Toliver-Kinsky**[3], and **Labros S. Sidossis**[1,4]

[1]Metabolism Unit, Shriners Hospitals for Children, Galveston, TX, USA

[2]Department of Surgery, University of Texas Medical Branch, Galveston, TX, USA

[3]Department of Anesthesiology, University of Texas Medical Branch, Galveston, TX, USA

[4]Department of Internal Medicine, University of Texas Medical Branch, Galveston, TX, USA

Abstract

Altered skeletal muscle mitochondrial function contributes to the pathophysiological stress response to burns. However, the acute and chronic impact of burn trauma on skeletal muscle bioenergetics remains poorly understood. Here, we determined the temporal relationship between burn trauma and mitochondrial function in murine skeletal muscle local to and distal from burn wounds.

Male BALB/c mice (8–10 weeks old) were burned by submersion of the dorsum in water (~95°C) to create a full thickness burn on ~30% of the body. Skeletal muscle was harvested from spinotrapezius underneath burn wounds (local) and the quadriceps (distal) of sham and burn treated mice at 3h, 24h, 4d and 10d post-injury. Mitochondrial respiration was determined in permeabilized myofiber bundles by high-resolution respirometry. Caspase 9 and caspase 3 protein concentration were determined by western blot.

In muscle local to burn wounds, respiration coupled to ATP production was significantly diminished at 3h and 24h post-injury ($P<0.001$), as was mitochondrial coupling control ($P<0.001$). There was a 5- ($P<0.05$) and 8-fold ($P<0.001$) increase in respiration in response to cytochrome at 3h and 24h post burn, indicating damage to the outer mitochondrial membranes. Moreover, we also observed greater active caspase 9 and caspase 3 in muscle local to burn wounds, indicating the induction of apoptosis. Distal muscle mitochondrial function was unaltered by burn trauma until 10d post burn, where both respiratory capacity ($P<0.05$) and coupling control ($P<0.05$) was significantly lower than sham.

Corresponding author: Craig Porter Ph.D. Metabolism Unit, Shriners Hospitals for Children – Galveston. Department of Surgery, University of Texas Medical Branch. Galveston, Texas, 77550. cr2porte@utmb.edu. P: 409-770-6676. F: 409-770-6674.

These data highlight a differential response in muscle mitochondrial function to burn trauma, where the timing, degree and mode of dysfunction are dependent on whether the muscle is local or distal to the burn wound.

Introduction

Altered mitochondrial function is a hallmark of the pathophysiological stress response to burns [1–11]. We recently demonstrated that skeletal muscle mitochondrial respiratory capacity and function were diminished at 2 and 3 weeks post-injury in humans with burns covering approximately 70% of the total body surface area (TBSA) [2]. In these patients, greater skeletal muscle mitochondrial thermogenesis was associated with profound hypermetabolism (increased metabolic rate) [2]. Further, we have recently reported similar findings in severely burned children, where altered mitochondrial function in skeletal muscle persists for up to two years post-injury [11]. Collectively, these data support a putative role for skeletal muscle mitochondrial thermogenesis in the hypermetabolic stress response to burns. In agreement with our findings in humans, Righi and colleagues reported greater TCA cycle flux but lower ATP production rates in murine skeletal muscle directly under burn wounds, suggesting a reduction in the coupling of TCA cycle flux to ATP production [12], indicative of mitochondrial uncoupling and thus thermogenesis.

An important difference in our human study [2] and the rodent study of Righi and colleagues [12] is the timing and site of muscle sampling. We biopsied tissue under the skin and from area which was not directly under full-thickness burn wounds from humans approximately 2 and 3 weeks post-injury [2]. In contrast, Righi *et. al*., [12] studied muscle directly under a comparatively small burn (5% TBSA) a matter of hours post injury. While we concluded that our data reflected a chronic adaptation where muscle mitochondria become uncoupled in response to burns in order to support thermoregulation [2], the data of Righi and co-workers [12] may reflect a more acute response to burn trauma, where reduced ATP production observed by these researchers may reflect apoptosis and/or mitophagy, at least in part. In support of this, Yashura and colleagues demonstrated altered mitochondrial membrane potential and release of mitochondrial cytochrome C into the cytosol as early as 15 min post burn in murine skeletal muscle harvested from under burn wounds [13]. Cytochrome C activates cytosolic caspase enzymes responsible for apoptosis [14]. Indeed, from 6h to 7d post injury, Yashura *et. at.*, [13] showed that caspase 3 activity was augmented in skeletal muscle directly beneath burn wounds, suggesting acute alterations in skeletal muscle mitochondrial function following direct burn trauma reflect an apoptotic response.

It appears that there may be differential acute and chronic effects of burn injury on skeletal muscle bioenergetics, which may be broadly characterized as an acute response to the blunt trauma of full-thickness burns, followed by a more chronic adaption in skeletal muscle mitochondria to the systemic milieu accompanying a large burn. Here, we set out to delineate the acute and chronic impact of severe burn trauma on skeletal muscle mitochondrial function local to and distal from full-thickness burn wounds. Our working

hypothesis is that the timing and nature of altered bioenergetics of muscle underlying burn wounds will be distinct from that of skeletal muscle distal to burn wounds.

Materials and methods

Animal procedures

We used a murine model of full-thickness burn trauma in the current study [15–18]. Similar to humans, hypermetabolism has been documented in similar murine models of burn trauma [19]. All animal experiments were performed in line with the National Institutes of Health guidelines on the use of animals for research. This study was approved by the Institutional Animal Care and Use Committee at the University of Texas Medical Brach.

Briefly, male BALB/c mice (8–10 weeks old) were housed on a 12:12 light:dark cycle at 24–26°C throughout the study period. Following the administration of buprenorphine (0.1 mg/kg i.p.), mice were anesthetized by inhalation of a 3–5% isoflurane mixture and remained fully anesthetized throughout the surgical procedure. Approximately 40% of the dorsum was shaved with electrical clippers before ~ 1cc of lactated ringers (LR) was injected s.c. in both burn and sham treated animals to protect the spinal column. Thereafter, the dorsum of burn treated animals was exposed to ~95°C water for 10 sec in a custom made cast to produce a full-thickness scald wound covering approximately 25–30% of the TBSA. Both burn and sham treated mice were then resuscitated with and i.p. injection of 1–2 cc of LR. All mice were housed individually following burn or sham treatment. Cohorts of mice were sacrificed at 3h, 24h, 4d and 10d post injury. The spinotrapezius muscle directly under burn wounds and the quadriceps muscle group distal to burn wounds were excised from burn and sham treated animals for biochemical analysis.

Tissue analysis

Skeletal muscle samples were split into three portions following collection from animals. One portion of tissue from both the spinotrapezius and the quadriceps was immediately placed in an ice-cold mitochondrial preservation buffer containing 10mM CaK_2-EGTA; 7.23mM K_2-EGTA; 20mM imidazole; 20mM taurine 50mM K-MES; 0.5mM dithiothreitol; 6.56 $MgCl_2$; 5.77mM ATP and 15mM creatine phosphate (pH of 7.1). This tissue was transferred to the laboratory for mitochondrial respiration measurements. The remaining muscle tissue was frozen in liquid nitrogen and stored at −80°C for future western blot analysis or fixed in 10% formalin for histochemical analysis.

Muscle fiber preparation

Approximately ten mgs of skeletal muscle was permeabilized by agitating myofiber bundles in 2mls of mitochondrial preservation buffer containing 20μM saponin at 4°C for approximately 30 min. Thereafter, myofiber bundles were washed in 2mls of mitochondrial respiration buffer containing 0.5mM EGTA; 3mM $MgCl_2$; 60mM K-lactobionate; 20mM taurine; 10mM KH_2PO_4; 20mM HEPES; 110mM sucrose; 1mg/ml essential fatty acid free bovine serum albumin (pH 7.1) at 4°C for approximately 15 min. Then, approximately 2 to 4mgs of myofiber bundles were blotted on filter paper and weighed on a precision micro-balance (Mettler-Toledo, Zaventem, Belgium) prior to being transferred to an Oxygraph-

O2K respirometer chamber (Oroboros Instruments, Innsbruck, Austria) where they were suspended in 2mls of mitochondrial respiration buffer. Respiration measurements were made on the same day as sample collection, typically within 6h of harvest.

High-resolution respirometry

Each day, an instrumental calibration was performed on polygraphic oxygen sensors at air saturation. Zero and instrumental background calibrations were performed using dithionite titrations at regular intervals throughout the study period to monitor instrumental stability. During experiments, temperature was maintained at 37°C and O_2 concentration within the range of 250–400 nmol/ml. Mitochondrial O_2 flux was computed and recorded at 2–4 sec intervals by DatLab software (Oroboros Instruments, Innsbruck, Austria).

Mitochondrial respiratory capacity and function were assayed in permeabilized skeletal muscle samples by the addition of saturating concentration of substrates (1.5mM octanoyl-l-carnitine, 5mM pyruvate, 2mM malate, 10mM glutamate and 10mM succinate) followed adenosine diphosphate (ADP, 5mM), cytochrome C (10μM) and the mitochondrial uncoupler carbonyl cyanide *m*-chlorophenyl hydrazone (CCCP) to a final concentration of 5μM. A schematic overview of the respiration protocol employed in the current study is presented in Figure 1. Mass specific state 2, state 3 and state 3_U respiratory fluxes are considered maximal since substrates are provided in excess. Coupled respiration correlates well with mitochondrial volume density in skeletal muscle [20], while we have shown a near linear relationship between state 3 and state 3_U respiration in skeletal muscle [21], suggesting that both maximal coupled (state 3) and uncoupled (state 3_U) respiration correlate with mitochondrial volume density in skeletal muscle. The sequential titration of substrates, ADP, cytochrome C and CCCP allowed leak respiration, coupled respiration, mitochondrial membrane intactness, and respiratory capacity, respectively to be assayed concurrently within the same sample. This protocol took approximately 60–90 min to complete. The respiratory control ratio (RCR) for ADP, which provides and index of mitochondrial coupling control was calculated by dividing state 3 (coupled) respiration by state 2 (leak) respiration, providing an index of mitochondrial quality per organelle. The RCR for cytochrome C was calculated by dividing state 3 respiration after cytochrome C titration by state 3 respiration prior to cytochrome C titration. Typically, cytochrome C titration has a minimal impact of respiratory fluxes. However, an increase in respiration of more than 10% (or a RCR >1.1) suggests damage to the outer mitochondrial membrane, where cytochrome C can enter the intra-membrane space and directly stimulate respiration. The leak control ratio (LCR), a marker of mitochondrial thermogenic capacity was calculated as state 2 respiration divided by maximal state 3_U respiration. Finally the flux control ratio (FCR), a marker of the efficiency of the oxidative phosphorylation system was calculated by dividing state 3 respiration by maximal state 3_U respiration. Since the denominator of in the LCR and FCR is state 3_U respiration, i.e., maximal respiration, both of these ratios fall within the confines of 0–1 [22–24] and can be considered as measures of mitochondrial membrane proton conductance (LCR) and oxidative phosphorylation efficiency (FCR) per mitochondrion, since they are normalized to the capacity of the electron transfer system.

Histology

Formalin fixed muscle samples were embedded in paraffin and sectioned for Hematoxylin and Eosin (H+E) staining. Image capture was performed using an Olympus BX41 light microscope (Olympus Corporation, NJ). All images shown are at 20X magnification. All *post hoc* cropping and adjustments for brightness/contrast and color tone where performed identically on all sample images to allow direct comparison.

Western Blot analysis

Active caspase 9 and active caspase 3 proteins were separated by SDS-polyacrylamide gel electrophoresis (PAGE) and transferred to nitrocellulose membranes. First, muscle samples were homogenized and proteins extracted using T-PER tissue extraction reagent (Thermo Scientific, Rockford, IL). Twenty micrograms of extracted protein from spinotrapezius and quadriceps muscles from sham, 24h post-burn and 10d post-burn animals were loaded into 4–12 % Bis-tris gels (Life Technologies, Carlsbad, CA). Gels were run in NuPAGE 2-(N-morpholino)ethanesulfonic acid - sodium dodecyl sulfate (MES-SDS) buffer (Life Technologies, USA) for 120 minutes at 100 V using X-SureLock Mini-Cell electrophoresis system (Life Technologies, Carlsbad, CA). Proteins were then transferred to a nitrocellulose membrane using transfer-buffer (Life Technologies, Carlsbad, CA) containing 20 % methanol at 30 V for two hours. Blots were blocked using 5 % (w/v) nonfat milk (BioRad, Hercules, CA) in TBS for 1 hour at room temperature. Membrane blots were then incubated with the following proteins of interest; active caspase 9 (abcam®, Cambridge, MA) at 1:300 dilution, cleaved caspase 3 (Cell signaling, USA) at 1:700 dilution and GAPDH antibody (SIGMA, St. Louis, MO) at 1:10,000 dillution in TBS containing 0.1 % Tween 20 (TBST) at 4°C overnight. Blots were washed three times with TBST for ten minutes each before probing with either donkey anti-rabbit secondary horseradish peroxidase (HRP) conjugates antibody (abcam®, Cambridge, MA) at 1:3000 dilution for one hour at room temperature. Blots were then washed with TBST, and visualized with autoradiography after incubation of blots in Pierce ECL Western blotting Substrate (Thermo Scientific, Rockford, IL) for 1 minute at room temperature according to the manufacturer's instruction. Autoradiographs were then scanned and band areas were measured using ImageJ 1.48 software (NIH, Bethesda, MD).

Statistical analysis

All data is presented as group means ± the standard error. Statistically significant differences were detected between sham/burn groups by means of a 1-way analysis of variance with a Tukey's multiple comparisons test. Statistical analysis was performed using GraphPad Prism Version 6 (GraphPad, La Jolla, CA).

Results

Skeletal muscle mitochondrial respiratory capacity

Mitochondrial respiration data is presented in Figure 2. State 2 (leak) respiration was significantly lower in the spinotrapezius muscle at 3h (17.2±5.1 pmol/s/mg; $P<0.05$) and 24h (9.2±2.3 pmol/s/mg; $P<0.001$), post-burn when compared to sham treated animals

(33.9±3.7 pmol/s/mg). At 4d (21.5±3.4 pmol/s/mg) and 10d post-burn (27.8±4.2 pmol/s/mg) leak respiration was no longer statistically different to the sham group (Figure 2A). Leak respiration was significantly greater in the 10d post-burn group compared to the 24h post-burn group (P<0.001). In contrast to the spinotrapezius muscle, leak respiration was not significantly altered by burn injury in the quadriceps muscle (Figure 2B).

State 3 (coupled) respiration (mitochondrial respiration *coupled* to ATP production) in the spinotrapezius and quadriceps muscles are shown in Figure 2C and 2D, respectively. Coupled respiration was significantly lower in the spinotrapezius muscle at 3h (11.7±3.0 pmol/s/mg; P<0.001), 24h (8.5±2.3 pmol/s/mg; P<0.001), and 4d (33.5±7.6 pmol/s/mg; P<0.05), post-burn when compared to sham treated animals (63.9±6.6 pmol/s/mg). Coupled respiration was significantly greater at 10d post-burn (44.2±7.2 pmol/s/mg; P<0.05) when compared to the 3h post-burn group (P<0.05) and the 24h post-burn group (P<0.01). Burn trauma had no effect on coupled respiration in quadriceps muscle at 3h, 24h or 4d post-burn. However, state 3 respiration was significantly lower at 10d post-burn (29.8±4.1 pmol/s/mg) when compared to the sham group (56.9±2.4 pmol/s/mg; P<0.05) and the 3h post-burn group (62.7±710.1 pmol/s/mg; P<0.05).

State 3_U respiration following the titration of the uncoupler CCCP, which reflects the maximal respiratory capacity of the electron transfer chain, is presented in Figure 2E (spinotrapezius) and 2F (quadriceps). Respiratory capacity was significantly lower in the spinotrapezius muscle at 3h (40.3±34.2 pmol/s/mg; P<0.05), 24h (36.6±8.6 pmol/s/mg; P<0.05), and 4d (37.5±6.4 pmol/s/mg; P<0.05), post-burn when compared to sham treated animals (69.7±4.5 pmol/s/mg). Respiratory capacity was not significantly different in the spinotrapezius at 10d post-burn (49.9±7.6 pmol/s/mg) when compared to the sham group. In the quadriceps, respiratory capacity was not different at 3h, 24h and 4d post-burn vs. sham. However, respiratory capacity was significantly lower at 10d post-burn (33.7±10.6 pmol/s/mg) vs. the sham (66.8±2.5 pmol/s/mg; P<0.05) and the 3h (72.5±10.2 pmol/s/mg; P<0.01) post-burn groups.

Skeletal muscle mitochondrial coupling control

High-resolution respirometry and the sequential titration of substrates, ADP and uncouplers allow coupling/flux control ratios to be calculated [22–24]. Since these ratios are determined within the same tissue sample and thus mitochondrial pool, they provide an index of mitochondrial quality. The RCR for ADP in spinotrapezius and quadriceps muscle are presented in Figure 3A and 3B, respectively. The RCR for ADP was significantly lower in the spinotrapezius muscle at 3h (0.75±0.07; P<0.001), 24h (0.96±0.14; P<0.001), 4d (1.57±0.16; P<0.001) and 10d (1.56±0.09; P<0.001) post-burn compared to the sham group (2.75±0.24). Compared to the 3h post-burn group, the RCR for ADP was significantly greater at 10d post-burn (P<0.05), suggesting some recovery in mitochondrial coupling control in mitochondria of the spinotrapezius muscle (Figure 3A). The RCR for ADP was not altered by burn injury for up to 4d post-injury. At 10d post burn (1.36±0.09), the RCR for ADP was significantly lower than the sham group (1.91±0.12; P<0.01), suggesting a gradual decline in mitochondrial coupling control in the quadriceps muscle following burn injury (Figure 3B).

The LCR ratio expresses leak respiration as a function of respiratory capacity, and reflects the capacity of the mitochondrial membranes for proton conductance and thus the thermogenic potential of the mitochondria. In the spinotrapezius muscle (Figure 3C) the LCR was largely unaltered by burn trauma, although was significantly lower at 24h post burn (0.24±0.05; P<0.05) when compared to sham (0.45±0.04). Further, the LCR was greater at 4d (0.57±0.05; P<0.01) and 10d (0.57±0.03; P<0.01) when compared to sham. In the quadriceps muscle (Figure 3D) the LCR increased after burn injury, and was significantly greater at 10d post-burn (0.71±0.05) when compared to the sham (0.46±0.04; P<0.05) and 3h post-burn (0.39±0.03; P<0.01) groups, suggesting a gradual increase in thermogenic potential of quadriceps muscle mitochondria in response to burn injury.

The FCR for the spinotrapezius and quadriceps muscles are presented in Figure 3E and 3F respectively. The FCR expresses maximal coupled or ATP producing respiration as a function of mitochondrial electron transfer capacity, and thus provides an index of the efficiency of the oxidative phosphorylation system. The FCR was significantly lower in the spinotrapezius muscle at 3h (0.28±0.06; P<0.001) and 24h (0.24±0.08; P<0.001) post-burn compared to the sham group (0.83±0.04). Further, the FCR was greater at 4d (0.67±0.0.04; P<0.001) and 10d (0.78±0.05; P<0.001) post-burn when compared to the 3h post burn group. Furthermore, the FCR was significantly greater in the 4 and 10d post-burn groups when compared to the 1 day post burn group (P<0.001). In contrast to the spinotrapezius, FCR was similar across all groups in the quadriceps muscle (Figure 3F).

Mitochondrial cytochrome C response

The titration of reduced cytochrome C during respirometry analysis provides a measure of the intactness of the outer mitochondrial membranes. Typically an increase in respiration of not more than 10% is considered to mean that the outer mitochondrial membranes are largely intact. In the spinotrapezius muscle, cytochrome C increased respiration by 29.8±4.0 and 29.0±8.7 pmol/s/mg at 3h and 24h post-burn, respectively (Figure 4A). The RCR for cytochrome C was 4.65±1.17 and 8.38±3.32 at 3h and 24h hours post-burn, respectively, which were both significantly greater than the sham (1.01±0.01; P<0.001), 4d post-burn (1.02±0.05; P<0.001) and 10d post-burn (1.03±0.02; P<0.001), where there were negligible changes in respiration following cytochrome C titration (Figure 4A). These data indicate that the outer mitochondrial membranes of the spinotrapezius muscle are severely damaged at 3h and 24h post-burn. In the quadriceps muscle, there was no significant increase in respiration in response to cytochrome C titration in any group, thus there were no significant differences between groups (Figure 4B), suggesting that the mitochondrial membranes were largely intact in quadriceps muscle after burn.

H and E staining of samples from sham and burn treated mice demonstrated evidence of severe muscle fiber trauma and a loss of muscle protein content in the spinotrapezius muscle at 24h post burn (Figure 4C). In particular, there was a striking lack of eosin staining in the spinotrapezius muscle at 24h post burn, which appeared to have been restored at 10d post-burn. Moreover, at 24h post injury muscle fibers from the spinotrapezius appeared atrophied when compared to those from the quadriceps muscle of the same animals (Figure 4C and 4D). In addition, fibers within the spinotrapezius appeared to have lost their architectural

organization. Indeed, in contrast to the quadriceps, the spinotrapezius had many nucleated cells with little to no eosin staining (Figure 4D), again indicating that skeletal muscle underneath full-thickness burn wounds undergoes profound trauma.

In line with functional evidence of damaged mitochondrial membranes in skeletal muscle directly underneath burn wounds, and histological evidence of severe trauma to this muscle tissue, we observed a 30% increase in active caspase 9 protein concentration and a 5-fold increase in active caspase 3 protein concentration ($P<0.01$) at 24h post in the spinotrapezius muscle (Figures 4E and 4F). Induction of either active caspase 9 or 3 was not observed in the quadriceps muscle post-burn (Figure 4E and 4F).

To underscore the relationship between damage to mitochondria in muscle underneath full-thickness burns and a subsequent loss of bioenergetics function, we performed correlation analysis between the RCR for cytochrome C (a measure of how damaged the outer mitochondrial membranes are) and the FCR (a measure of the efficiency of the oxidative phosphorylation system). We found a significant correlation between these two parameters in the spinotrapezius muscle ($R= -0.80$, $P<0.001$; Figure 5A), indicating that when the mitochondrial membranes are damaged by burn trauma, mitochondrial flux control (i.e. the coupling of fuel oxidation to ATP production) is lost. Indeed, correlation analysis of the FCR and state 3 (coupled) respiration revealed a significant relationship between the mitochondrial efficiency (FCR) and the muscles respiratory capacity in the coupled state ($R= 0.84$, $P<0.001$; Figure 5B). Since the quadriceps were distal to burn wounds and therefore not subjected to direct trauma, mitochondria in these samples did not respond to cytochrome C. Thus, no correlation between the RCR for cytochrome C and the FCR was evident in the quadriceps (Figure 5C). Similarly, since the FCRs measured for quadriceps mitochondria were generally >0.80, suggesting >80% efficiency in oxidative phosphorylation, there was no evidence of a correlation between the FCR and coupled respiratory capacity in muscle distal to burn wounds (Figure 5D).

Discussion

Altered skeletal muscle mitochondrial function is a hallmark of the pathophysiology of severe burn trauma [1, 2, 4, 11, 12, 25]. However, the nature of this altered function, and the temporal relationship between burn trauma and altered skeletal muscle bioenergetics remain poorly understood. Using a murine model of severe burn injury, we set out to determine the acute and chronic impact of severe burn trauma on mitochondrial function in skeletal muscle that is local to and distal from full-thickness burn wounds. We demonstrate distinct differences in the manifestation of altered skeletal muscle mitochondrial function in response to burn injury, depending on the locality of muscle to burn wounds. Specifically, in muscle local to burn wounds mitochondria exhibit an acute apoptotic response, whereas as in muscle distal to burn wounds we observed a chronic reduction in mitochondrial respiratory capacity and coupling control, where mitochondria exhibit a more thermogenic phenotype. Collectively, the current study sheds new light on the temporal and physiological nature of burn-induced alterations in skeletal muscle bioenergetics.

Mitochondrial respiratory capacity, whether in the leak, coupled or uncoupled state, was markedly diminished almost immediately post-injury in skeletal muscle local to full-thickness burn wounds. This depression in respiratory capacity was most apparent at 24h post injury, and had begun to return towards values seen in sham animals at 4d and 10d post-burn. Interestingly, the loss in respiratory capacity was not as great as the loss in the capacity for coupled ATP producing respiration at 3h and 24h post burn, suggesting that while some capacity for mitochondrial electron transfer and respiration is maintained in muscle local to burn wounds, capacity for oxidative phosphorylation is all but completely lost. In support of this assertion, we also observed acute alterations in mitochondrial coupling control in muscle local to burn wounds. Specifically, the RCR for ADP was less that one at 3h and 24h post burn (Figure 3A), meaning mitochondria were completely uncoupled. Similarly, the FCR, a measure of mitochondria oxidative phosphorylation efficiency, was approximately 75% lower at 3h and 24h post-burn when compared to sham in muscle local to burn wounds. These data suggest that mitochondria within skeletal muscle local to burn wounds were moribund or dead in terms of capacity for oxidative phosphorylation at 3h and 24h post-injury.

In stark contrast to muscle local to burn wounds, mitochondrial respiratory capacity was unaltered in skeletal muscle distal to burn wounds for up to 4d post-injury. However, at 10d post-burn coupled respiration (phosphorylation) and uncoupled respiration (respiratory capacity) were both significantly lower than the sham cohort. Similarly, with regards to indices of intrinsic mitochondrial function, we observed no evidence of altered mitochondrial quality within the first 4d post-injury in muscle distal to burn wounds. At 10d post-injury, in addition to diminished respiratory capacity, we also observed a significantly lower ADP RCR (Figure 3B) and LCR (Figure 3D), suggesting a reduction in mitochondrial phosphorylation capacity and an increase in mitochondrial thermogenic capacity, respectively, in muscle distal to burn wounds. These data suggest a more subtle alteration in mitochondrial respiratory capacity and function in muscle distal do burn wounds. Given that this response does not present till the second week after injury, we postulate that it may reflect both an adaptation in mitochondrial coupling, towards a more thermogenic phenotype, which may also be compounded by muscle wasting and denervation after burn trauma.

Collectively, our data clearly demonstrate a dichotomy in mitochondrial responses to burn trauma within skeletal muscle, which are dependent on whether muscle is local to or distal from full-thickness burn wounds. Our findings are in agreement with others who have shown that there is approximately a 76% reduction in ATP production rates in murine skeletal muscle directly under a 5% TBSA burn at 6h post injury, which was accompanied by a 50% reduction in ATP availability in burned skeletal muscle [12]. Further, the same group also reported a 96% reduction in mitochondrial ATP production at 3d post injury in muscle directly under burn wounds a mice with 5% TBSA burn [25]. Interestingly though, in this study, despite a near complete reduction in ATP production rates, ATP concentration within muscle tissue was actually around 13% greater in muscle under burn wounds compared to muscle from control mice [25], a finding which was close to statistical significance (P=0.06). Thus, it would appear that despite a near total capitulation in mitochondrial oxidative phosphorylation in muscle underlying full-thickness burn in the

initial few days post-injury, residual ATP production remains and appears sufficient to maintain muscle ATP levels.

Interestingly, while we show that mitochondrial respiratory capacity and coupling control are largely maintained for up to 4d post injury in muscle distal to burn wounds, Tzika and colleagues previously reported a 78%, 91% and 98% reduction in ATP production rate at 1d, 3d and 7d respectively, in skeletal muscle (hind-limb) distal to burn wounds in mice with 30% TBSA burns [4]. These findings are difficult to reconcile with our own current data. For example, the magnitude of the reduction of ATP production seen by Tzika and colleagues [4] in muscle distal to a large 30% TBSA burn wound at 1d, 3d and 7d post-injury is similar to the same groups observations in muscle directly underneath a comparatively smaller (5% TBSA) burn at 6h [12] and 3d [25] post-injury. While the aforementioned studies [4, 12, 25] determined ATP production *in vivo* using ^{31}P nuclear magnetic resonance spectroscopy, and we assayed mitochondrial respiratory capacity and function in the current study in permeabilized myofiber bundles using high-resolution respirometry, it is unlikely that the discrepancy observed in the data can be entirely attributable to methodological approaches.

Since high-resolution respirometry permits both mitochondrial capacity and intrinsic function to be determined concomitantly [22], the fact that we observe a concurrent reduction in respiratory capacity and function within the first 4d after injury in muscle local to burn wounds, but unaltered mitochondrial capacity or function in muscle distal to burn wounds over the same time period within the same animals, instills us with confidence that our own data is robust. Further, our findings in murine muscle distal to burn wounds are in line with our observation in humans with massive burns. Indeed, in adults with burns covering approximately 70% of their TBSA, while we see a 50% reduction in mitochondrial respiration linked to ATP production, around 30% of maximal respiration was still sensitive to the ATP synthase inhibitor oligomycin in these patients [2], which we conclude to mean that skeletal muscle mitochondria retain some capacity for oxidative phosphorylation following severe burns. Physiologically, this make sense since skeletal muscle protein synthesis and breakdown are significantly elevated in burn survivors for months if not years post-injury [26–29], meaning that despite being largely immobilized in the acute period after injury, resting muscle ATP turnover is likely greater in muscle of burn survivors [30]. Indeed, cross-limb studies suggest that in patients with burns over 40% of the TBSA, O_2 consumption is 50% greater than skeletal muscle of healthy individual [31]. While we suggest that much of this increase in muscle O_2 consumption supports and increase in mitochondrial thermogenesis following burn trauma [2, 11], given that several ATP consuming reaction increase in skeletal muscle in response to burn trauma, it is likely that a significant proportion of this increase in basal O_2 consumption supports oxidative phosphorylation.

A further line of evidence supporting distinct responses of mitochondria in muscle local to and distal to burn wounds are our cytochrome C responses data. The introduction of reduced cytochrome C into respiration buffer should illicit little or no respiratory response if mitochondria have intact outer membranes. This approach is typically used to demonstrate that the preservation and preparation of samples for mitochondrial function assays did not

inadvertently lead to the lysing of organelles. Here, we have exploited this approach to demonstrate that mitochondria in muscle directly underlying full-thickness burns are traumatized, i.e., their outer membranes have been damaged by local burn trauma. Indeed, a respiratory response to cytochrome C was observed in muscle local to burn wounds at 3h and 24h post-injury. Thus, in the first 24h after burn in muscle directly under full-thickness burn wounds, mitochondrial membranes are severely damaged, which explains our respirometry data where these mitochondria have diminished respiration but in particular, are completely uncoupled. Indeed, we found a significant correlation in the response of mitochondrial to cytochrome C and the mitochondrial flux control in the spinotrapezius muscle only. This suggests the response to cytochrome C in the spinotrapezius reflects damage to the mitochondrial membranes and a subsequent inability to generate and utilize membrane potential.

In an attempt to ascribe a physiological role to the apparent loss in mitochondrial membrane intactness in muscle beneath burn wounds, the abundance of key proteins involved in cell apoptosis were measured. The release of endogenous mitochondrial cytochrome C into the cell cytosol activates caspase 9, which in turn cleaves caspase 3, a key mediator of programmed cell death (apoptosis) into its biologically active form [14]. We observed an induction in both active caspase 9 and in particular its down-stream effector caspase 3 at 24h post-injury only in muscle local to burn wounds. Whether this induction of apoptosis observed here was the result of lysis of the mitochondrial membranes or opening of mitochondrial transition pore on the outer mitochondrial membranes was not determined in the current study. Nevertheless, we provide evidence that apoptosis accompanies the acute derangements in mitochondrial function seen in muscle underneath full-thickness burn wounds, whereas the chronic alterations in skeletal muscle mitochondrial function following burn trauma are not associated with cellular apoptosis. Furthermore, our current data are in good agreement with that published in the literature, where acute burn trauma results in a depletion of mitochondrial cytochrome C and increase caspase 3 activity in muscle tissue underneath burn wounds [13]. Moreover, our histological analysis of tissue directly under burn wounds suggest muscle fiber atrophy and a profound loss in intracellular protein, indicative of cell death acutely post-injury in muscle local to full-thickness burn wounds.

To summarize, we set out to concurrently determine the temporal impact of burn trauma on mitochondrial function in skeletal muscle local to and distal from full-thickness burn wounds. To the best of our knowledge, we report for the first time that acute and chronic alterations in skeletal muscle mitochondrial function are dependent on the localization of burn wounds. Perhaps not surprisingly, despite retaining respiratory capacity, mitochondria local to burn wounds lose much their capacity for oxidative phosphorylation acutely post-injury; a response appeared to be mediated by a loss in the ability to generate mitochondrial membrane potential, which was accompanied by the induction of apoptosis. Contrastingly, muscle distal to burn wounds exhibited an altered phenotype post-injury consistent with a chronic reduction in phosphorylation capacity and a concomitant increase in thermogenic capacity. To conclude, these data demonstrate a differential response of muscle mitochondria to burn trauma, and suggest that the time of interventions aimed at altering mitochondrial function following burn trauma will likely influence efficacy.

Acknowledgments

We thank Geping Fang for assisting in animal care and husbandry. This work was funded by Shriners of North America research grants to L.S.S (84090 and 85310), T.T.K (85300), CS (85800), D.N.H (80500), and the morphology and pathology core facility at Shriners hospitals for Children – Galveston (84060). Support was also provided by the Institute for Translational Sciences at the University of Texas Medical Branch, supported in part by a Clinical and Translational Science Award (UL1TR000071) from the National Center for Advancing Translational Sciences, National Institutes of Health. CP was supported in part by a postdoctoral research fellowship from the National Institute of Disability and Rehabilitation Research (H133P110012).

References

1. Cree MG, Fram RY, Herndon DN, Qian T, Angel C, Green JM, et al. Human mitochondrial oxidative capacity is acutely impaired after burn trauma. Am J Surg. 2007; 196:234–9. [PubMed: 18639661]
2. Porter C, Herndon D, Borscheim E, Chao T, Reidy P, Borack M, et al. Uncoupled skeletal muscle mitochondria contribute to hypermetabolism in severely burned adults. Am J Physiol Endocrinol Metab. 2014; 307:462–7.
3. Porter C, Herndon D, Sidossis L, Børsheim E. The impact of severe burns on skeletal muscle mitochondrial function. Burns. 2013; 39:1039–47. [PubMed: 23664225]
4. Tzika A, Mintzopoulos D, Padfield K, Wilhelmy J, Mindrinos M, Yu H, et al. Reduced rate of adenosine triphosphate synthesis by in vivo 31P nuclear magnetic resonance spectroscopy and downregulation of PGC-1beta in distal skeletal muscle following burn. Int J Mol Med. 2008; 21:201–8. [PubMed: 18204786]
5. Wang X, Chen K, Shi Y, Shi H. Functional changes of the NADH respiratory chain in rat-liver mitochondria and the content changes of high-energy phosphate groups in rat liver and heart during the early phase of burn injury. Burns. 1990; 16:377–80. [PubMed: 2275769]
6. Wang X, Yang L, Chen K. Catecholamines: important factors in the increase of oxidative phosphorylation coupling in rat-liver mitochondria during the early phase of burn injury. Burns. 1993; 19:110–2. [PubMed: 8471141]
7. Wang X, Zhu L, Yang L, Miao M, Chen K, Liu S. Activity changes of ATP synthase and adenylate kinase in rat-liver mitochondria during the early phase after burn injury. Burns. 1995; 21:362–3. [PubMed: 7546259]
8. Hu H, Greif R, Goodwin C. The effects of thermal injury on mitochondrial oxygen consumption and the glycerol phosphate shuttle. Metabolism. 1994; 43:913–6. [PubMed: 8028518]
9. Jeschke M, Gauglitz G, Song J, Kulp G, Finnerty C, Cox R, et al. Calcium and ER stress mediate hepatic apoptosis after burn injury. J Cell Mol Med. 2009; 13:1857–65. [PubMed: 20141609]
10. Aprille J, Hom J, Rulfs J. Liver and skeletal muscle mitochondrial function following burn injury. J Trauma. 1977; 17:279–88. [PubMed: 192906]
11. Porter C, Herndon D, Børsheim E, Bhattarai N, Chao T, Reidy P, et al. Long-Term Skeletal Muscle Mitochondrial Dysfunction is Associated with Hypermetabolism in Severely Burned Children. J Burn Care Res. 2015 Epub ahead of print.
12. Righi V, Constantinou C, Mintzopoulos D, Khan N, Mupparaju S, LGR, et al. Mitochondria-targeted antioxidant promotes recovery of skeletal muscle mitochondrial function after burn trauma assessed by in vivo 31P nuclear magnetic resonance and electron paramagnetic resonance spectroscopy. FASEB J. 2013; 27:2521–30. [PubMed: 23482635]
13. Yasuhara S, Perez ME, Kanakubo E, Yasuhara Y, Shin YS, Kaneki M, et al. Skeletal muscle apoptosis after burns is associated with activation of proapoptotic signals. Am J Physiol Endocrinol Metab. 2000; 279:1114–21.
14. Elmore S. Apoptosis: a review of programmed cell death. Toxicol Pathol. 2007; 35:495–516. [PubMed: 17562483]
15. Bohannon J, Cui W, Sherwood E, Toliver-Kinsky T. Dendritic cell modification of neutrophil responses to infection after burn injury. J Immunol. 2008; 185:2847–53. [PubMed: 20679533]

16. Toliver-Kinsky T, Lin C, Herndon D, Sherwood E. Stimulation of hematopoiesis by the Fms-like tyrosine kinase 3 ligand restores bacterial induction of Th1 cytokines in thermally injured mice. Infect Immun. 2003; 71:3058–67. [PubMed: 12761083]

17. Toliver-Kinsky T, Varma T, Lin C, Herndon D, Sherwood E. Interferon-gamma production is suppressed in thermally injured mice: decreased production of regulatory cytokines and corresponding receptors. Shock. 2002; 18:322–30. [PubMed: 12392275]

18. Porter C, Herndon D, Bhattarai N, Ogunbileje J, Szczesny B, Szabo C, et al. Severe Burn Injury Induces Thermogenically Functional Mitochondria in Murine White Adipose Tissue. Shock. 2015; 44:258–64. [PubMed: 26009824]

19. Yo K, Yu Y, Zhao G, Bonab A, Aikawa N, Tompkins R, et al. Brown Adipose Tissue and Its Modulation by a Mitochondria-targeted Peptide in Rat Burn Injury Induced Hypermetabolism. Am J Physiol Endocrinol Metab. 2012; 304:331–41.

20. Larsen S, Nielsen J, Hansen CN, Nielsen LB, Wibrand F, Stride N, et al. Biomarkers of mitochondrial content in skeletal muscle of healthy young human subjects. J Physiol. 2012; 590:3349–60. [PubMed: 22586215]

21. Porter C, Reidy P, Bhattarai N, Sidossis L, Rasmussen B. Resistance exercise training alters mitochondrial function in human skeletal muscle. Med Sci Sports Exerc. 2014; 47:1922–31. [PubMed: 25539479]

22. Gnaiger E. Capacity of oxidative phosphorylation in human skeletal muscle: new perspectives of mitochondrial physiology. Int J Biochem Cell Biol. 2009; 41:1837–45. [PubMed: 19467914]

23. Gnaiger, E. An introduction to OXPHOS analysis. 4. OROBOROS MiPNet Publications; 2014. Mitochondrial pathways and respiratory control.

24. Pesta D, Gnaiger E. High-resolution respirometry: OXPHOS protocols for human cells and permeabilized fibers from small biopsies of human muscle. Methods Mol Biol. 2012; 810:25–58. [PubMed: 22057559]

25. Padfield K, Astrakas L, Zhang Q, Gopalan S, Dai G, Mindrinos M, et al. Burn injury causes mitochondrial dysfunction in skeletal muscle. Proc Natl Acad Sci U S A. 2005; 102:5368–73. [PubMed: 15809440]

26. Biolo G, Fleming RY, Maggi SP, Nguyen TT, Herndon DN, Wolfe RR. Inverse regulation of protein turnover and amino acid transport in skeletal muscle of hypercatabolic patients. J Clin Endocrinol Metab. 2002; 87:3378–84. [PubMed: 12107253]

27. Hart DW, Wolf SE, Chinkes DL, Gore DC, Mlcak RP, Beauford RB, et al. Determinants of skeletal muscle catabolism after severe burn. Ann Surg. 2000; 232:455–65. [PubMed: 10998644]

28. Hart DW, Wolf SE, Mlcak R, Chinkes DL, Ramzy PI, Obeng MK, et al. Persistence of muscle catabolism after severe burn. Surgery. 2000; 128:312–9. [PubMed: 10923010]

29. Chao T, Herndon D, Porter C, Chondronikola M, Chaidemenou A, Abdelrahman D, et al. SKELETAL MUSCLE PROTEIN BREAKDOWN REMAINS ELEVATED IN PEDIATRIC BURN SURVIVORS UP TO ONE-YEAR POST-INJURY. Shock. 2015 Epub ahead of print.

30. Yu YM, Tompkins RG, Ryan CM, Young VR. The metabolic basis of the increase of the increase in energy expenditure in severely burned patients. JPEN J Parenter Enteral Nutr. 1999; 23:160–8. [PubMed: 10338224]

31. Wilmore D, Aulick L. Systemic responses to injury and the healing wound. JPEN J Parenter Enteral Nutr. 1980; 4:147–51. [PubMed: 7401260]

Highlights

- Burn injury results in skeletal muscle mitochondrial dysfunction.
- Mitochondria local to wounds exhibit and apoptotic phenotype acutely post burn.
- Mitochondria distal to wounds undergo a chronic loss of respiratory capacity and function.
- Locality to burn wounds dictates the timing and mode of muscle mitochondrial dysfunction.

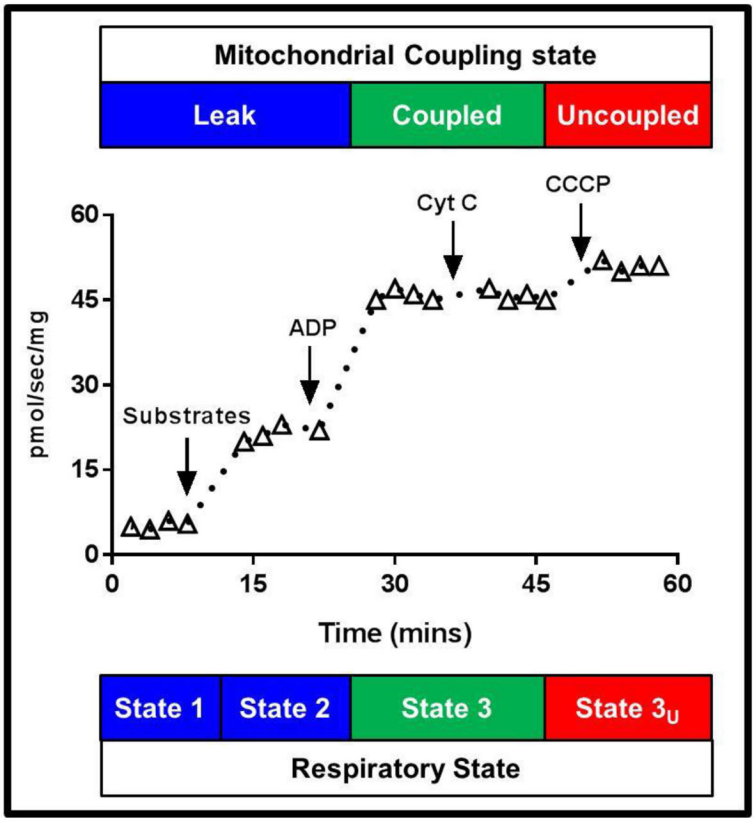

Figure 1.

A schematic overview of the mitochondrial respiration protocol used in the current study. Steady-state leak (state 2) respiration was determined after the titration of 1.5mM octanoyl-carnitine, 5mM pyruvate, 2mM malate, 10mM glutamate and 10mM succinate. Steady-state coupled (state 3) respiration was determined following the titration of 5mM ADP. The intactness of the outer mitochondrial membrane was then determined following the titration of 12μM cytochrome C. Finally, mitochondrial respiratory capacity (uncoupled state 3_U respiration) was determined following the titration of CCCP to a final concentration of 5μM.

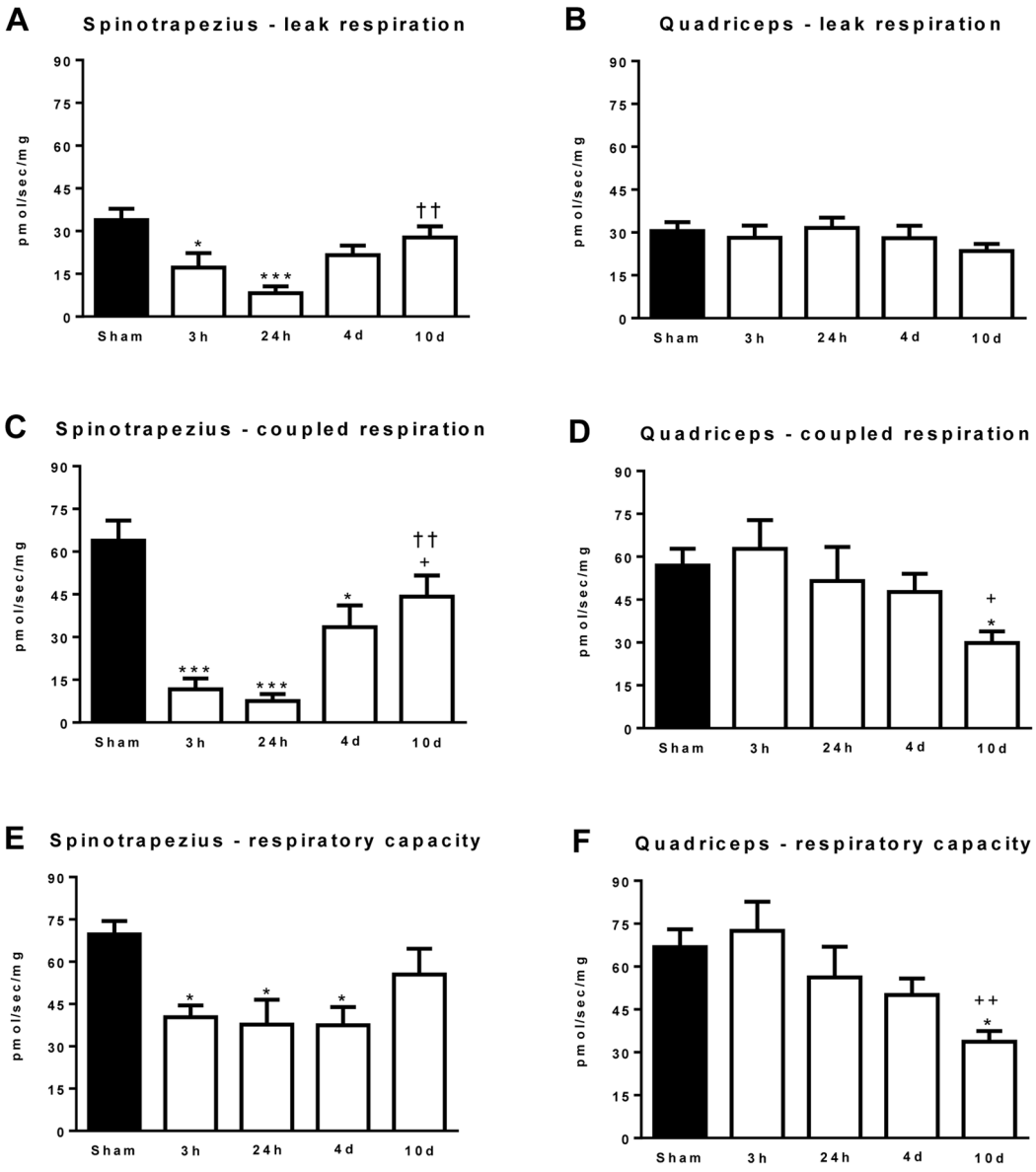

Figure 2.

(A) State 2 leak respiration in the spinotrapezius muscle. (B) State 2 leak respiration in the quadriceps muscle. (C) State 3 coupled respiration in the spinotrapezius muscle. (D) State 3 coupled respiration in the quadriceps muscle. (E) Respiratory capacity (uncoupled state 3_U respiration) in the spinotrapezius muscle. (F) Respiratory capacity (uncoupled state 3_U respiration) in the quadriceps muscle. Values are means ± the standard error. *P<0.05 and ***P<0.001 vs. sham. $^{+}$P<0.05 and $^{++}$P<0.01 vs. 3h post-burn. ††P<0.01 vs. 24h post-burn. *n*=5 to 8 animals per group.

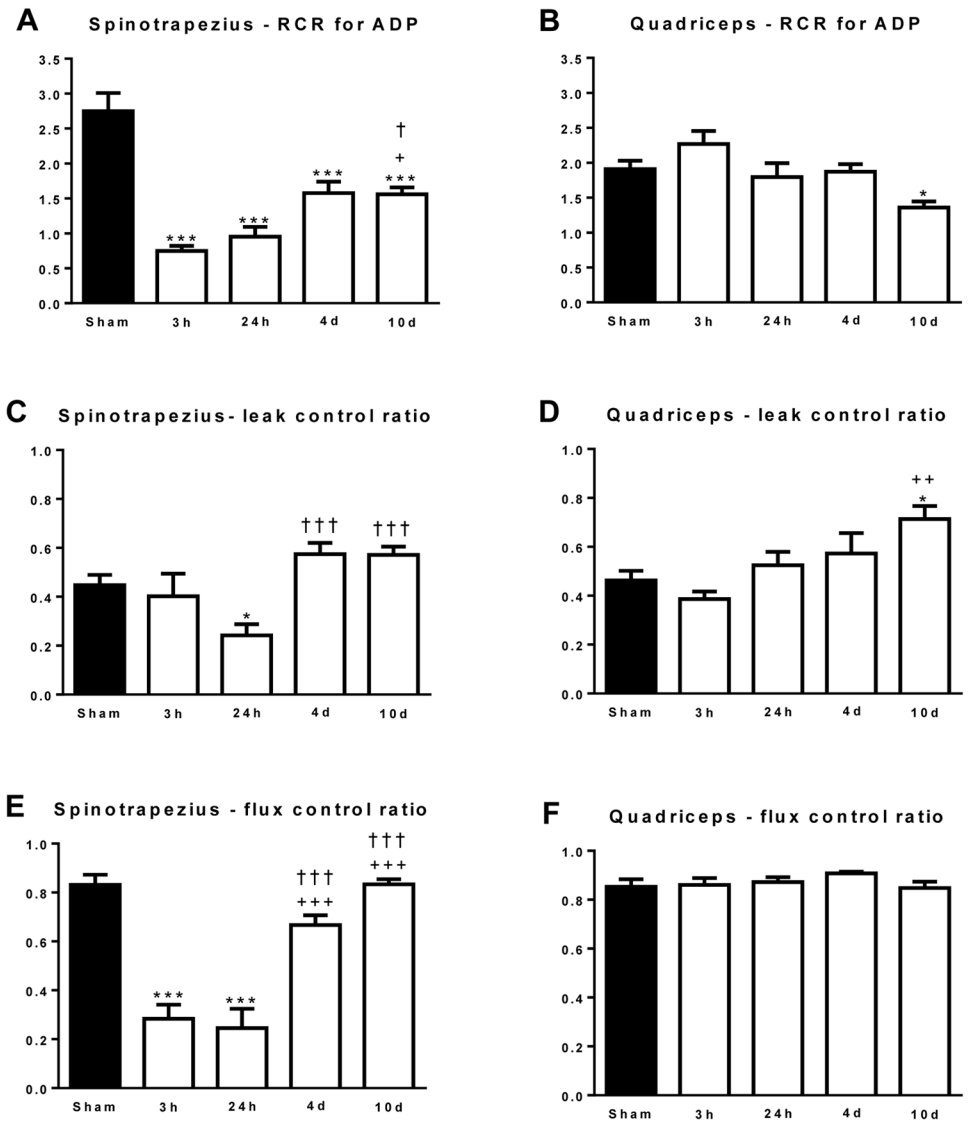

Figure 3.

(A) The respiratory control ratio (RCR) for ADP in the spinotrapezius muscle. (B) The RCR for ADP in the quadriceps muscle (C) The leak control ratio (LCR) in the spinotrapezius muscle. (D) The LCR in the quadriceps muscle. (E) The flux control ratio (FCR) in the spinotrapezius muscle. (F) The FCR in the quadriceps muscle. *P<0.05 and ***P<0.001 vs. sham. $^{+}$P<0.05, $^{++}$P<0.01 and $^{+++}$P<0.001 vs. 3h post-burn. †P<0.05 and †††P<0.001 vs. 24h post-burn. *n*=5 to 8 animals per group.

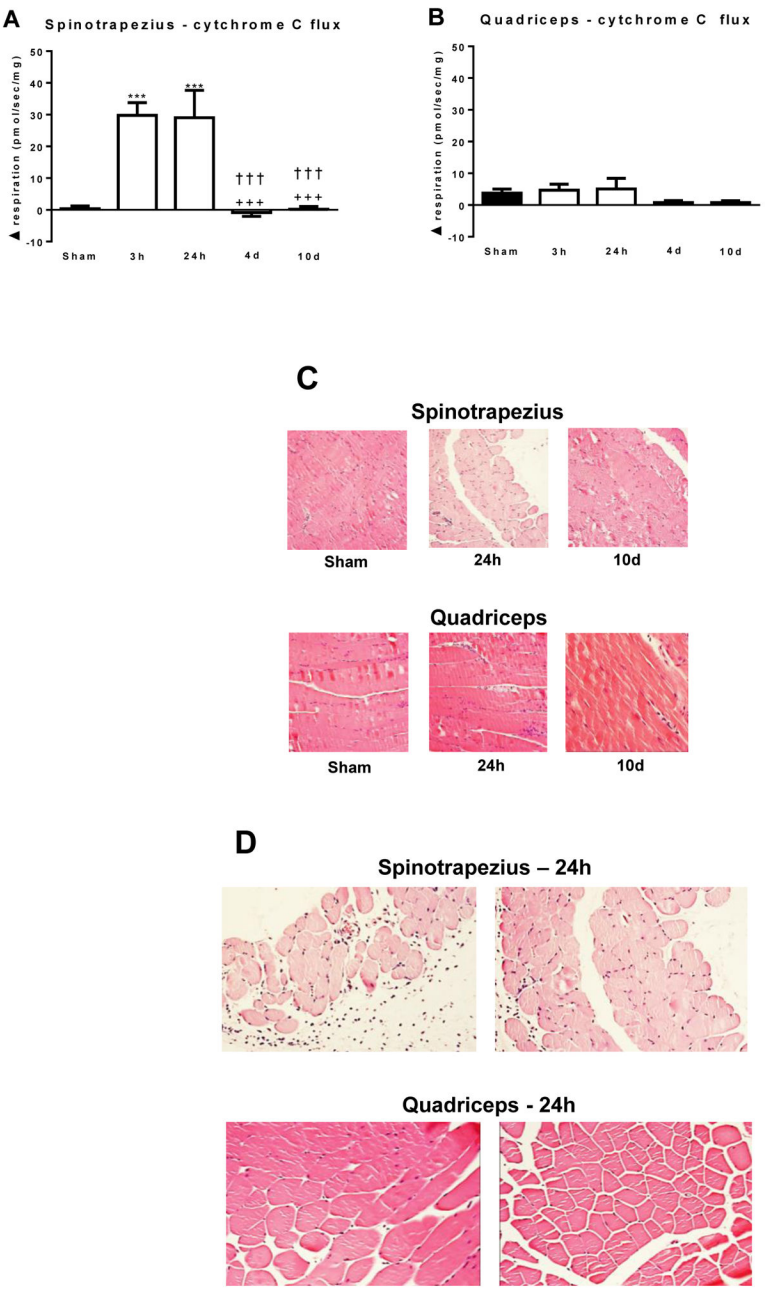

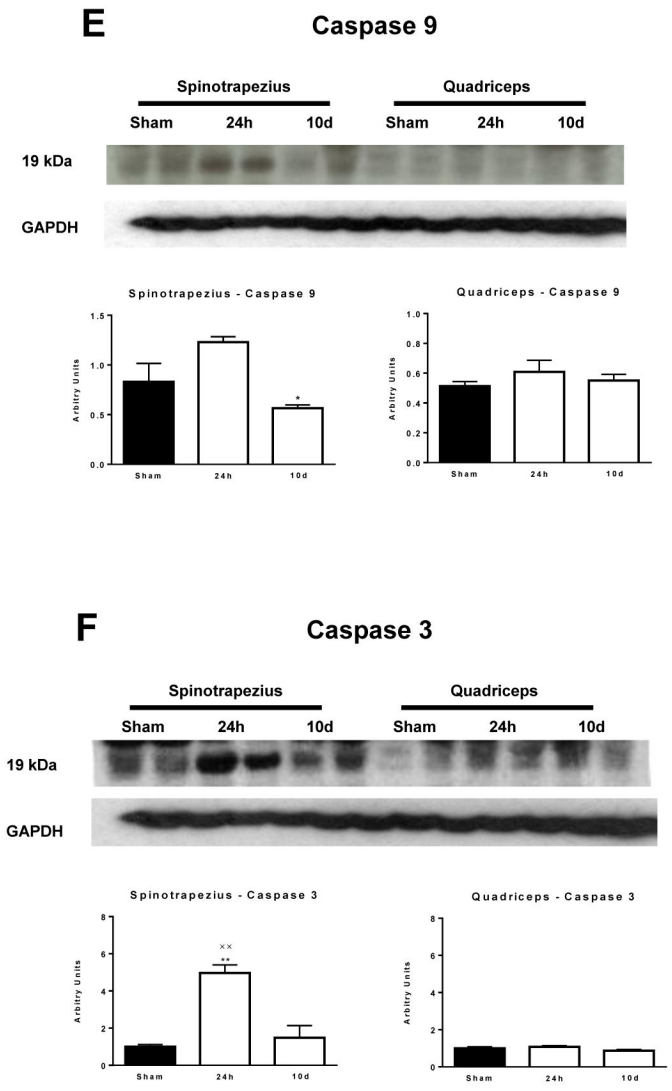

Figure 4.

The respiratory response to cytochrome C in the spinotrapezius (A) and quadriceps (B) muscle. (C) Representative 20X magnification H+E histology of spinotrapezius and quadriceps muscle from sham treated animals and burned animals at 24h and 10 days post-injury. (D) Representative 20X magnification H+E histology of spinotrapezius and quadriceps muscle from 2 sham and 2 burn treated animals at 24h post-injury. (E) Cleaved caspase 9 protein concentration in the spinotrapezius and quadriceps muscle. (F) Cleaved caspase 3 protein concentration in the spinotrapezius and quadriceps muscle. ***P<0.001 vs. sham. $^{+++}$P<0.001 vs. 3h post-burn. †††P<0.001 vs. 24h post burn. ^{xx}P<0.01 vs. 10d post burn. *n*=5 to 8 animals per group. Western blots images show two animals from each group on the same gel.

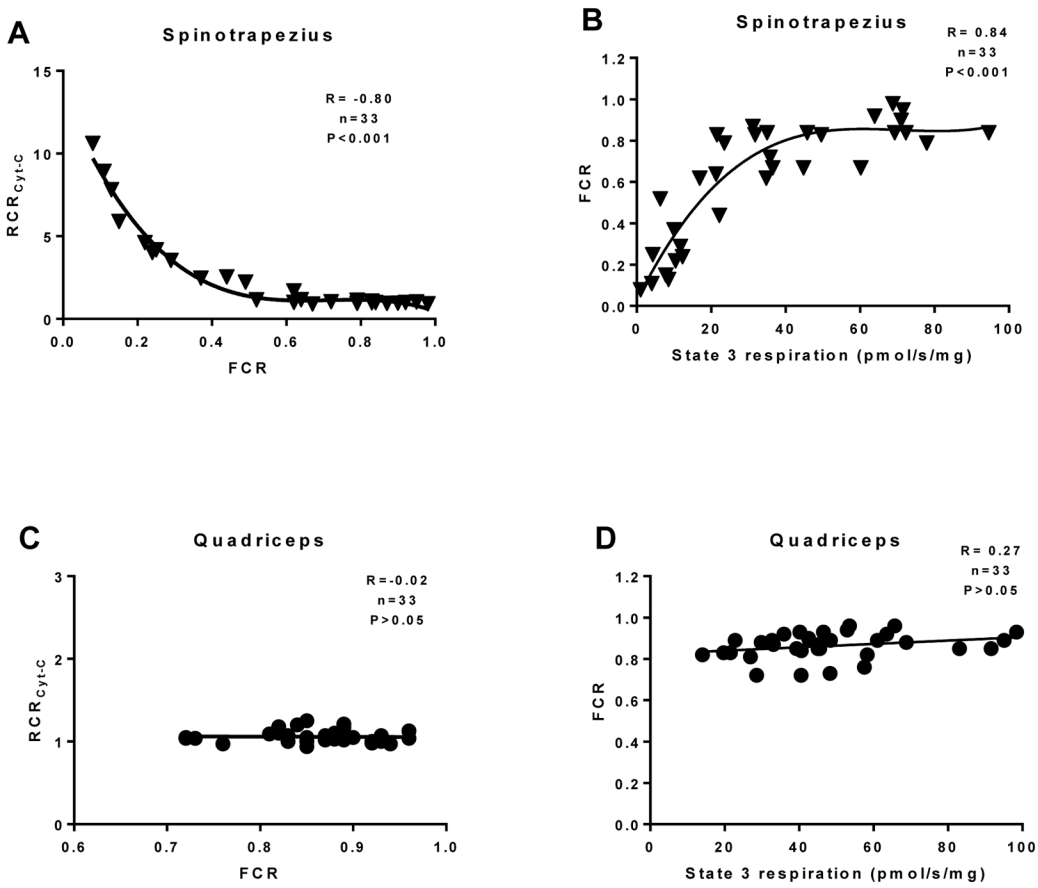

Figure 5.

Correlation analysis was performed between the RCR for cytochrome C and the FCR in the spinotrapezius (A) and quadriceps (C). Further, correlation analysis was performed between the FCR and coupled (state 3) respiration in the spinotrapezius (B) and quadriceps (D). A non-parametric Spearman correlation was performed in A and B, while a Pearson correlation was performed in C and D. Non-linear third order polynomial lines of best fit are shown in A and B. The slope of the linear regression is shown in C and D.